Revue Roumaine de Chimie, **2006**, *51*(3), 169–178

BIOLOGICALLY ACTIVE Cu(II) AND Fe(III) COMPLEXES OF A PHENOTHIAZINE DERIVATIVE WITH AN EXTENDED COORDINATION SPHERE. SOLUTION STRUCTURES

Cornelia G. PALIVAN,[a] Elena BÂCU,[b] Simona ANTONESCU,[c*] Cornelia GURAN[c] and Georg GESCHEIDT[d]

[a] University of Basel, Department of Chemistry, Klingelbergstrasse 80, 4056 Basel, Switzerland
[b] University "Al. I. Cuza", Faculty of Organic Chemistry, Carol I 11, 700506 Iasi, Roumania
[c] University "Politehnica", Faculty of Industrial Chemistry, Polizu 1, 011061 Bucharest, Roumania
[d] Graz University fo Technology, Institute for Physical and Theoretical Chemistry, Technikerstr. 4/I, A-8010, Austria

Received July 15, 2005

Copper and iron complexes of N-[α- benzoyl-amino-β-(10-methyl-3-phenothiazinyl)-acriloyl]-phenylhydrazine were prepared and dissolved in DMF. The corresponding solution structures were established using EPR and electronic spectroscopy. In the case of the copper complexes various four-co-ordinate Cu(II) species with distorted square-planar geometry around the metal ion are established, while two high-spin Fe^{3+} species with octahedral co-ordination and different rhombicity have been put into evidence for the iron complexes. The solution structures are compared with the analytical data of the parent complexes in the solid state.

INTRODUCTION

Considerable emphasis has been placed on the detailed study of metal complexes with biologically active molecules because of their postulated involvement in a range of biological and catalytic processes where the metal is considered to play an important role.[1,2] Phenothiazine derivatives display a large variety of pharmacological effects (neuroleptic, antiemetic, antiinflammatory, antimicotic, antitumor activity) and for this reason the parent heterocycle, its derivatives as well as the corresponding metal complexes have been studied both *in vivo* and *in vitro*.[3-6] Generally, the formation of metal complexes leads to an increase of the mutagenic activity.[7]

In this study we try to establish in how far the co-ordination sphere around the metal in copper and iron complexes of N-[α-benzoyl-amino-β-(10-methyl-3-phenothiazinyl)-acriloyl]-phenylhydrazine (**L**) (Fig. 1) is modified upon dissolution in DMF. How does the side-chain participate in the co-ordination? Is the phenothiazine part involved in the metal co-ordination? Is this arrangement stable upon dissolution in a co-ordinating solvent, as DMF?

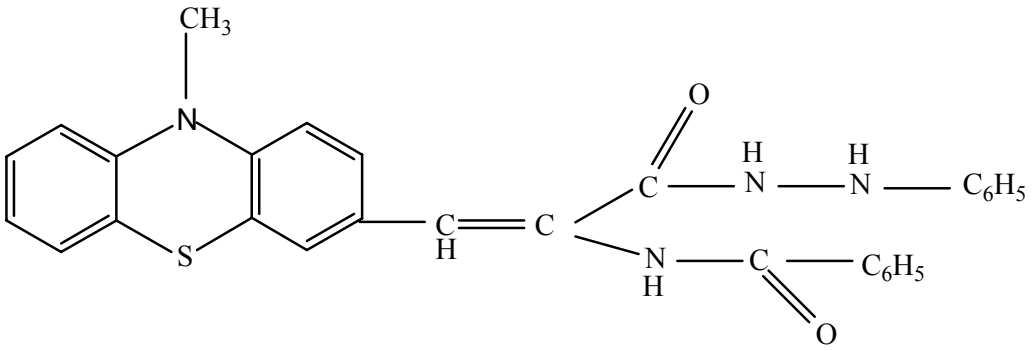

Fig. 1 – Structure of **L** phenothiazine derivative used as ligand.

* Corresponding author: simona_pasolescu@yahoo.com

The starting point is the solid state structure of the complexes obtained by analytic methods. The first-order co-ordination sphere of the metal was established by optical spectroscopy and EPR which provide insight into the changes that the metal complex undergo upon dissolution in a solvent. EPR and optical spectroscopy[8-10] have proven to be powerful techniques for studying the molecular structure of the paramagnetic complexes in the solid state as well as the structural changes that they may undergo upon dissolution in a solvent.[11]

The *in vitro* tests have shown greater antibacterial activity of these complexes compared with the parent ligand (on *Coryn. diphteriae*, *Strept. fecalis*, *Bacillus cereus*, *Escherichia coli*),[12] therefore the metal co-ordination geometry could be related to their biological behaviour.

RESULTS AND DISCUSSION

Complexes in solid state

The infrared spectra of the investigated complexes can give insight especially on the co-ordination manner of **L**. For all complexes the ν_{N-H} stretching vibration, bathochromic shifts have been observed in comparison with the free ligand (from 3250 cm^{-1} to 3215-3235 cm^{-1} for all the complexes). The N-N vibration frequency (ν_{N-N}) has a slight hypsochromic shift compared with the value of free ligand **L** (from 930 cm^{-1} to 935-945 cm^{-1}). The $\nu_{C(arom/aliph)-N}$ frequency is shifted from 1245 to 1210-1225 cm^{-1} in the case of complexes **III** – **V**. No shift was observed for the $\nu_{C=O}$ frequency (1680 cm^{-1}) for all the complexes, compared to the free ligand. Therefore we consider that **L** acts as a bidentate chelating ligand involving 2 N atoms in the coordination sphere, one from phenylhydrazine and the other one from the benzoyl-amino part of the molecule.

The presence of a significant fine structure and splitting in the domain of strong ClO^-_4 vibrations, near 1100cm^{-1} is due to the coordination of perclorate ions, in the case of complex **III.** [13, 32, 33]

The electronic spectra of the complexes **I** contains a large band at 625 nm ($^2E \rightarrow {}^2T_2$) specific for the distorted tetrahedral geometry around Cu^{2+}.[14]

The shift of the absorption band to ≈800 nm in the case of complex **II** is probably due to the dinuclear metal complex character.

The electronic spectra of the complexes **IV** and **V** present a single large band at 512-570 nm and 392-416 nm, respectively, which could be assigned to a spin forbidden d-d transition but also to a charge transfer transition specific for Fe^{3+} in octahedral surrounding. Generally these bands lie at fairly high energies and are superposed.

The polycrystaline EPR spectra of the copper complexes at room temperature are isotropic in overall shape. The calculated g_{iso} values are: 2.164 (complex **I**), 2.166 (complex **II**), 2.175 (complex **III**). They did not change by lowering the temperature at 77K, therefore a static behaviour of the geometry around the metal is assumed.

The polycrystalline EPR spectra of the iron complexes are isotropic and very broad (approx. 800 G linewidth) that correspond to a g of 2.014 (complex **IV**) and 2.017 (complex **V**), respectively. There is an additional signal, of low intensity, with a gyromagnetic factor of 4.34.

Complexes in solution

According to the conductivity measurements, all complexes have a nonelectrolyte nature, indicating the presence of anion moieties (Cl^- or ClO_4^-) in the inner of the co-ordination sphere.

The electronic spectra of complexes **I** and **II** in DMF solutions are similar and show a very strong absorption band around 380 nm that corresponds to LMCT transitions. The broad band in the region 600-850 nm is attributable to the d-d transitions of the metal ion and its maximum located around 670 nm indicates a tetrahedrally distorted square-planar arrangement around copper.[15,16] On dissolution of the complex **II** in DMF, the ligand-field spectral features are quite different, indicating a change in the structure in solution, compared with the solid state structure.

In the case of complex **III** there is a strong absorption at 373 nm with a shoulder around 500 nm, and they are due to LMCT transitions. In addition, a d-d absorption around 600 nm appears, suggesting a CuN_2O_2 chromophore in distorted square-planar arrangement to the copper.[15]

The chloro complexes **I** and **II** show a d-d band at longer wavelengths than the perchlorate complex **III**, as found in other copper complexes having the anions participating in the co-ordination sphere.[17]

The frozen solution EPR spectra of complexes **I-III** (Fig. 2) at 77 K show that more than one paramagnetic species are present due to the lineshape signal in the parallel region (Fig. 3). The values of the EPR parameters for complexes **I-III** presented in Table 2 indicate that the unpaired electron is located in a ground state orbital of type $d_{x^2-y^2}$ or d_{xy}, due to the $g_{zz} > g_{xx} \cong g_{yy} > 2.004$ relation and that all the paramagnetic species have four-co-ordinate structures.[18]

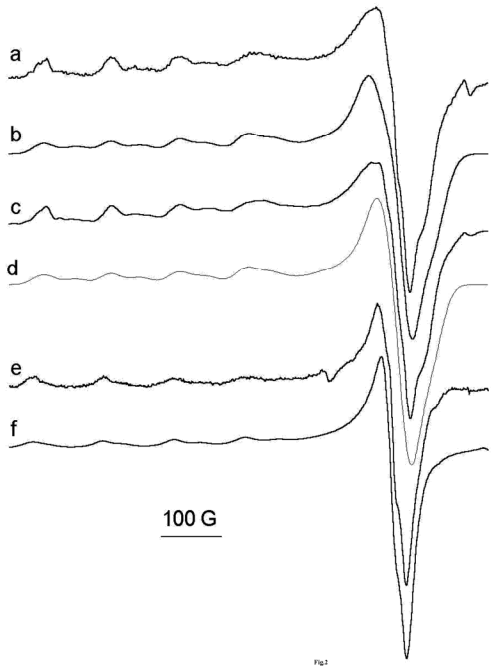

Fig. 2 – Frozen solution EPR spectra of copper complexes **I**, **II** and **III** (a, c and e, respectively) together with their simulations (b, d, and f, respectively) according the EPR parameters from Table 1.

Table 1

Spin Hamiltonian parameters for Cu(II) complexes in DMF at 77°K. **Γ** represents the linewidth tensor on which the simulations were based

Comp	**g**		**A**^{Cu} [mT]		A_{iso} [mT]	**Γ** [mT]		
	$g_\perp$	$g_{\|\|}$	$A_\perp$	$A_{\|\|}$		$\Gamma_\perp$		$\Gamma_{\|\|}$
I A	2.061	2.349	1.57	10.74	4.90	2.5	2.7	2.8
I B	2.082	2.391	1.45	11.28	5.04	2.3	2.3	2.3
II A	2.062	2.350	1.58	10.82	4.93	2.5	2.5	2.5
II B	2.079	2.392	0.92 1.04	11.20	4.71	1.9	2.0	2.0
III A	2.079	2.365	0.34	0.37 12.84	4.86	1.6	1.6	2.3
III B	2.080	2.400	0.51	0.51 11.91	4.68	1.6	1.6	2.5

The half-field measurements performed in order to see if there are dimers showed that only the spectrum of complex **III** presents a very weak signal connected with the $\Delta m_s = \pm 2$ transition. For the other complexes, even if the microwave power was increased up to 80 mW and multiple acquisitions were done, the half-field transition did not appear at 77 K.

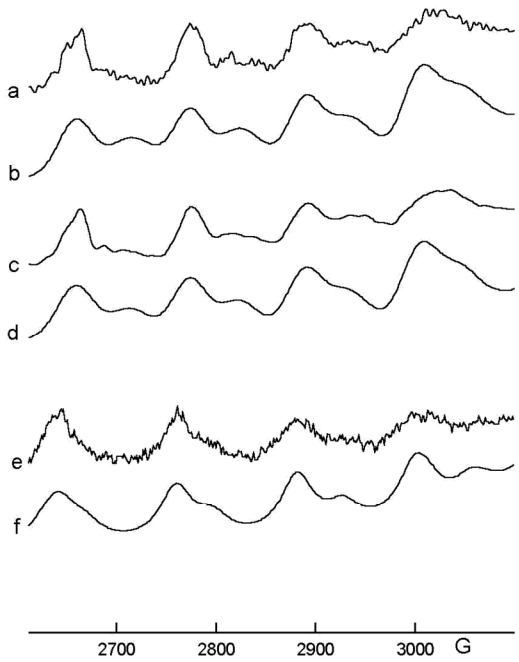

Fig. 3 – Parallel region of frozen solutions EPR spectra for copper complexes **I**, **II** and **III** (a, c and e, respectively) together with their simulations (b, d, and f, respectively).

The comparison of the EPR parameters from complexes **I** and **II** shows that the major species (species **IA** and **IIA**, respectively) have similar parameters and therefore we assume an identical first sphere co-ordination around copper for both complexes.

According to the EPR parameters and the conductivity measurements, the first co-ordination sphere around copper in species **IA** consists in $2N_2Cl$ in a tetrahedral distorted square-planar geometry, similar to published data.[11] This lets us consider that the major component have the bidentate ligand still participating in the co-ordination of copper. Therefore in complex **I** the solid state form was not changed significantly by dissolution. This is supported by similar ligand-field spectral features in the absorption spectra of the solid and fluid samples.

The tetrahedral distortion from a square planar geometry that characterises species **IA** is indicated by an increase of the g_{zz} value together with a decrease of the A_{zz} value, greater towards a tetrahedral arrangement,[19] as for example in the case of Cu type I proteins where $A_{zz}<10.0$ mT.[20] This is supported by the position of the d-d band in the absorption spectrum, that represents an indicator of the transformation from a square-planar to tetrahedral stereochemistry.[16]

For complex **II**, species **IIA**, the major component, indicates that the dimer present in the solid state does not persist in the presence of DMF. During dissolution it changes into a form that corresponds to that of **I**, as reported for other copper dimers when they are dissolved in co-ordinating solvents (alcohol, DMF, pyridine).[2]

The species **B,** as a minor component in these complexes, has a $CuCl_2O_2$ co-ordination around copper and this indicates that a replacement of the ligand by DMF, in a low proportion, has to be taken into account.

The spectrum of complex **III** has a shape due to more than one paramagnetic species, too. The major species (**IIIA**) has EPR parameters that can be related with a $2N_2O$ co-ordination around copper in a tetrahedral distorted square-planar symmetry.[31] They are quite different compared with those of species **IA** and **IIA**. The difference has to be attributed to the participation of the counterions in the inner co-ordination sphere, as has been already seen for other copper complexes having phenothiazine derivatives as ligands.[29] Moreover, the greater A_{zz} value of this species together with the blue shift of the d-d band are indicating a less distorted tetrahedral arrangement around copper than in the case of complex **I**.

We suppose that the minor component **IIIB** with 4O in the first sphere co-ordination of copper, is due to the participation of DMF, by replacing the ligand, in very low proportion.

The fluid solution EPR spectra of complexes **I** and **III** (Fig. 4) can be simulated by taking into account a major component (species **IA** and **IIIA**) and one minor component (species **IB** and **IIIB**), while in the case of complex **II** only one component (**IIA**) is established (Table 2).

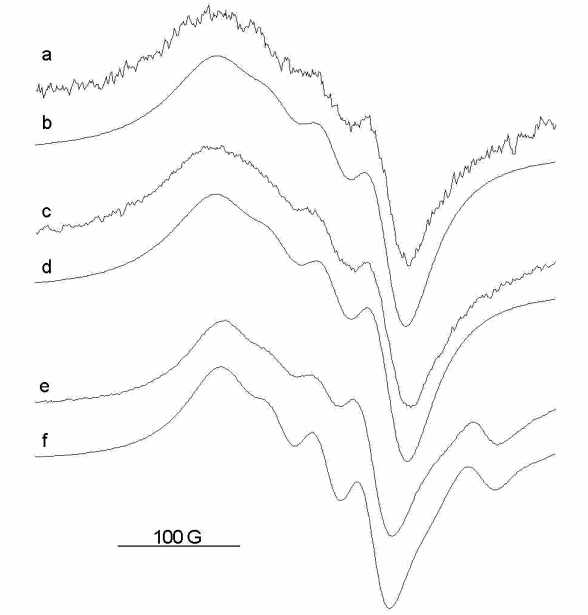

Fig. 4 – Fluid solution EPR spectra of copper complexes **I**, **II** and **III** (a, c and e, respectively) together with their simulations (b, d, and f, respectively) according to the EPR parameters from Table 2.

Table 2

Spin Hamiltonian parameters for Cu(II) complexes in DMF at 295°K. a, b, c are the linewidth parameters in the equation (1)

Comp	g_{iso}	A_{iso} [mT]	a	b	c
I A	2.179	3.96	48.0	7.2	0.9
I B	2.067	0.84	6.6	0.1	1.7
II	2.179	4.02	47.0	6.9	0.9
III A	2.178	3.57	38.0	4.9	1.1
III B	2.138	5.60	33.0	10.9	0.1

The species **IA-IIIA** present in fluid solutions have significantly smaller A_{iso} values than in the frozen solutions, while the g_{iso} values are only slightly increased. This illustrates aggregation phenomena due to the freezing process.[21]

The species **IIIB** present as minor component points to the participation of DMF in the co-ordination, as we discussed in the case of the frozen solution. The EPR parameters of species **IC** are very different compared with the isotropic values obtained from the frozen solution measurements (species **IB**), therefore an additional conversion of complex **I** has to be taken into account.

Ligand field calculations

The ligand field calculations are a simple way to obtain the covalence coefficients for the major component of these complexes by assuming a D_{2d} symmetry around the metal (Table 3). Factor α^2, arising from the dipole-dipole interaction between the magnetic moments associated with the spin motion of the electron and the nucleus, has been shown to decrease when the delocalisation of the unpaired electron on the neighbouring atoms is increasing. The minimum theoretical value for a completely covalent bond is 0.5 and

increases until an ionic bond is formed, when a value of 1 is predicted. In our case all the complexes show enough strong covalency, their α^2 values being lower than 0.86. The complexes have a significant degree of covalency both of the in-plane π bonds (β_1^2 coefficient) and of out-of-plane π bonds (β'^2 coefficient). They show a rather significant delocalisation of the unpaired electron into 4s orbitals of the ligands, too, as can be seen from the values of γ'^2. This analysis indicates that species **IA** as a major component of the mixture in the case of complexes **I** and **II** has a distorted tetrahedral symmetry around copper, greater than species **IIIA**.

Table 3

Computed covalence coefficients and k values, by assuming for the copper complexes a D_{2d} symmetry (only the major paramagnetic species **A** was taken into account)

Comp.	k	α^2	β^2	γ^2	α'^2
I A	0.40	0.757	0.879	0.670	0.080
II	0.41	0.755	0.878	0.666	0.081
III A	0.37	0.855	0.948	0.813	0.048

The EPR parameters obtained for these Cu complexes are very different from those reported for an unsubstituted phenothiazine Cu(II) complex[2] where the nitrogen atom of phenothiazine is directly involved in the co-ordination of the metal. Therefore it seems that the presence of the metal ion is biologically significant, and induces an increase of the parent phenothiazine derivative activity, a direct co-ordination to the phenothiazine nitrogen atom not being required.

Iron complexes

As the conductivity measurements show, the complexes have a nonelectrolyte nature and this can be connected with the presence of the Cl^- anion in the inner of the co-ordination sphere.

The electronic spectra of complexes **IV** and **V** show a band at 390 nm with a shoulder around 500 nm that are assigned to LMCT transitions. It is expected that for a d^5 configuration, the absorption spectra give no information because the tail of the intense charge-transfer absorption overlaps the weak forbidden bands of the visible region, producing the yellow colour. However, for both complexes a very weak band at 850nm appears and can be assigned as a $^6A_1 \rightarrow {}^4T_1$ transition of octahedrally co-ordinated high-spin Fe(III).[22]

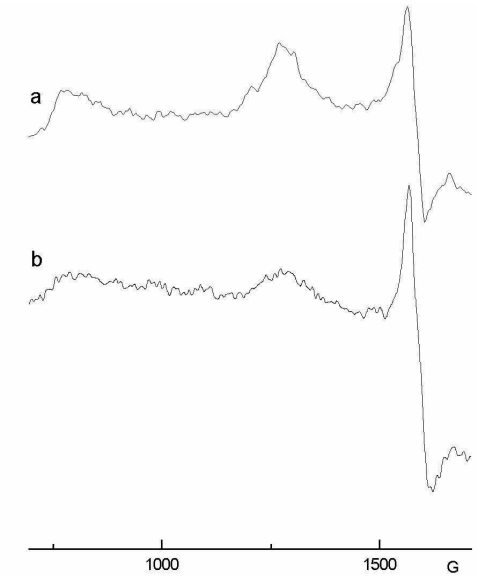

Fig. 5 – Frozen solutions EPR spectra of iron complexes **IV** and **V** (a and b, respectively).

The frozen solution EPR spectra of complexes I**V** and **V** (Fig. 5) are similar in terms of their shape and consist of three signals: one intense near g = 4.3 and two at lower magnetic field (at ca. 1275G, and 780G). The difference between them is a greater intensity for the latter absorptions in the case of complex I**V** compared with those of complex **V**. The experimental g_{eff} values are presented in Table 4.

Using the spin Hamiltonian formalism for high-spin iron(III),[23] the low field resonances can be assigned to two species **A** and **B**, with different rhombic (E/D) distortions.

Species **IVA** and **VA** are characterised by the well-resolved EPR signal near g = 4.3, specific for a transition between the middle Kramer doublet of a rhombically distorted high-spin iron(III) complex.[22] It is the most dominant spectral feature and is specific of near-perfect rhombicity, characterised by the ratio E/D = 1/3, as predicted by the Maltempo model[24] for the first excited doublet of a pure high-spin state. The narrow linewidth of the signal is another feature showing that the complexes can be characterised by a pure rhombic crystal field, being known that when a distortion from pure rhombic to axial geometry takes place, a broadening or a splitting of this line will take place.[22]

Table 4

Spin Hamiltonian parameters for Fe(III) complexes in DMF at 77°K

Comp.	g_{eff}	E/D
IVA	4.285	0.33
IVB	5.314 8.660	0.12
VA	4.260	0.33
VB	5.318 8.715	0.13

The weaker resonances at g ~ 8,7 and g ~5.3 were assigned to a second high-spin iron(III) species **IVB** and **VB**, respectively. These species have a S = 5/2 ground state subject to zero-field splitting that resolves the 6-fold degeneracy into three Kramer/s doublets with predominant spin character: (1/2), (3/2) and (5/2). If the separation of the doublets is large compared to βH and if the electron spin relaxation is sufficiently slow, each doublet is expected to give rise to its own resonance which can be described in terms of an effective S = ½ spectrum with three effective g values, not all observed. The resulting nine g values depend on the E/D ratio.[23] The g values obtained for **IVB** and **VB** can be fairly well reproduced by rhombicity parameters E/D indicating significant distortions from the axial symmetry, as have been previously found in other iron(III) complexes.[25] Moreover, as in our iron(III) complexes the low-field absorptions are similar with those for $[Fe(L)Cl_3]$ complexes,[26] we assume that the Cl atoms participate in the co-ordination sphere of iron.

The fluid solution EPR spectra for both complexes show a very intense isotropic signal with g_{iso} of 2.0166 for complex **IV** and 2.0168 for complex **V**, characteristic for a high-spin d^5 iron(III) system.[27]

The formation of the high-spin configuration in the case of the iron complexes[25] as well as the presence of monomeric copper species for the copper complexes in solutions are supposed to be a consequence of the weak-field nature of the ligand **L**.

EXPERIMENTAL PART

Synthesis

The synthesis of the ligand N-[α-benzoyl-amino-β-(10-methyl-3-phenothiazinyl)-acriloyl]-phenylhydrazine (**L**) was described previously.[28] The copper and iron complexes were obtained in a similar manner to the earlier procedure.[6,29] The methanol solutions of the metal salts and the ligand were refluxed for 3-4 h. For all the complexes, the resulting precipitates were isolated by filtration after solvent evaporation, washing in methanol-ether mixture and drying on $(P_2O_5)_2$ dessicator. All chemicals were of reagent grade and used after purification with appropriate procedures.

CAUTION! Perchlorate salts can be potentially explosive during drying and grinding. So proper care should be taken while handling such compounds. So far we have not experienced any problems during the preparation of samples.

Analytical characterisation of the complexes

The complexes were characterised by elemental analysis (N, Cu, Cl), electronic spectra (VSU-2G spectrophotometer using MgO as standard sample for solid state measurements, and in DMF solution, at 25°C), IR spectra (Perkin-Elmer spectrophotometer using KBr pellets) and molar electrical conductivity (in DMF solution at 25°C with OK 102/1 Radelkis Conductometer).

The analytical results along with values and assignments for the principal IR frequencies and the electronic transitions are presented below:

Complex I: [Cu**L**Cl_2] Yield: 87%; M = 627.1; m.p.> 300° C
Experimental: N 9.14%, Cu 10.49%, Cl 11.11%. Calculated: N 8.93%, Cu 10.13%, Cl 11.32%.
IR :$\nu_{(C-N)}$ = 1240 cm^{-1}, $\nu_{(NH)}$ = 3230 cm^{-1}, $\nu_{(Cu-N)}$ = 420 cm^{-1}, $\nu_{(C=O)}$ = 1680 cm^{-1}, $\nu_{(Cu-Cl)}$ = 290 cm^{-1}, $\nu_{(N-N)}$ = 940 cm^{-1}.
Electronic spectrum: λ≈625 nm (large band) with shoulder at 689 nm.
Electronic spectrum of DMF solution: λ = 380 nm and a large band at λ ≈ 600-850 nm.
Molar electrical conductivity: 12 μS cm^{-1}.

Complex II: [Cu_2 **L**Cl_4 $(OH_2)_2$] Yield: 83%; M = 797.6; m.p.> 300° C
Experimental: N 7.15%, Cu 15.43%, Cl 17.36%. Calculated: N 7.02%, Cu 15.93%, Cl 17.80%.
IR :$\nu_{(C-N)}$ = 1245 cm^{-1}, $\nu_{(NH)}$ = 3235 cm^{-1}, $\nu_{(Cu-N)}$ = 420 cm^{-1}, $\nu_{(C=O)}$ = 1680 cm^{-1}, $\nu_{(Cu-Cl)}$ = 290 cm^{-1}, $\nu_{(N-N)}$ = 935 cm^{-1}.
Electronic spectrum: λ ≈ 800 nm (large band) with a shoulder at 910 nm.
Electronic spectrum of DMF solution: λ = 383 nm and a large band at λ ≈ 600-850 nm.
Molar electrical conductivity: 27 μS cm^{-1}.

Complex III: [Cu**L**$(ClO_4)_2$] Yield: 89%; M = 755.1; m.p.> 300° C
Experimental: N 7.15%, Cu 8.10%, S 4.20%. Calculated: N 7.42 %, Cu 8.41%, and S 4.24%.
IR :$\nu_{(C-N)}$ = 1220 cm^{-1}, $\nu_{(NH)}$ = 3220 cm^{-1}, $\nu_{(Cu-N)}$ = 425 cm^{-1}, $\nu_{(C=O)}$ = 1680 cm^{-1}, $\nu_{(Cu-O)}$ = 490 cm^{-1}, $\nu_{(N-N)}$ = 945 cm^{-1}, ν_{ClO4-} = 1106 cm^{-1}.
Electronic spectrum: λ ≈ 840-910 nm (large band).
Electronic spectrum of DMF solution: λ = 373 nm with a shoulder at 500 nm; λ = 600 nm.
Molar electrical conductivity: 38 μS cm^{-1}.

Complex IV: [Fe**L**Cl_3OH_2] Yield: 88%; M = 673.1; m.p.> 300° C
Experimental: N 8.63%, Fe 8.48%, Cl 15.74%. Calculated: N 8.32 %, Fe 8.31%, and Cl 15.82%.
IR :$\nu_{(C-N)}$ = 1225 cm^{-1}, $\nu_{(NH)}$ = 3215 cm^{-1}, $\nu_{(Fe-N)}$ = 430 cm^{-1}, $\nu_{(C=O)}$ = 1680 cm^{-1}, $\nu_{(Fe-Cl)}$ = 490 cm^{-1}, $\nu_{(N-N)}$ = 935 cm^{-1}.
Electronic spectrum: λ ≈ 512 nm (large band) with a shoulder at 571 nm.
Electronic spectrum of DMF solution: λ = 385 nm with a shoulder at 500 nm; λ = 850 nm.
Molar electrical conductivity: 26 μS cm^{-1}.

Complex V: [Fe_2 **L**Cl_6 $(OH_2)_4$] Yield: 75%; M = 889.6; m.p.> 300° C
Experimental: N 6.46%, Fe 12.73%, Cl 11.73%. Calculated: N 7.42 %, Fe 12.59%, and Cl 11.91%.
IR :$\nu_{(C-N)}$ = 1220 cm^{-1}, $\nu_{(NH)}$ = 3220 cm^{-1}, $\nu_{(Cu-N)}$ = 425 cm^{-1}, $\nu_{(C=O)}$ = 1680 cm^{-1}, $\nu_{(Fe-Cl)}$ = 490 cm^{-1}, $\nu_{(N-N)}$ = 945 cm^{-1}.
Electronic spectrum: λ ≈ 392 nm (large band) with shoulder at 416 nm.
Electronic spectrum of DMF solution: λ = 390 nm with a shoulder at 500 nm; λ = 850 nm.
Molar electrical conductivity: 17 μS cm^{-1}.

EPR spectroscopy

The complexes were measured as powder without any treatment after the synthesis, and as DMF solutions (the concentration of copper(II) in solutions amounting to 0.1–0.5 x10^{-3} mol/dm^3).

EPR spectra were recorded either at ambient temperature or at 77°K in liquid nitrogen, in quartz finger dewar, with an EPR Bruker ESP300 X-band spectrometer. All the spectra were recorded using 100 kHz modulation frequency and microwave power of 2–4 mW. Optimisation of spectral resolution was achieved by making multiple acquisition (25 scans) and using fast Fourier transformation with a Gaussian profile for subsequent noise reduction. DPPH was used as a field marker (g = 2.0036).

All spectra were simulated using Symfonia software Bruker[30] based on a third order perturbation theory treatment. The ^{63}Cu/^{65}Cu isotopes in their natural abundance were considered for each spectrum.

In order to characterise the delocalisation of the unpaired electron, the covalence coefficients were calculated in a D_{2h} model symmetry, using a simple LCAO-MO calculus.[31] The spin-orbit coupling constants of the ligands λ_L, were included in the model, because of their large values (as λ_{Cl} = 586cm^{-1}, for example).

CONCLUSION

The interest of the present study was to establish in how far the solvent DMF enters into the co-ordination sphere of some Cu and Fe complexes with N-[α-benzoyl-amino-β-(10-methyl-3-phenothiazinyl)-acriloyl]-phenylhydrazine as ligand. The starting point was the preparation of five complexes in the solid state followed by their characterisation by analytical methods. Then the solution structure of the complexes in DMF was inspected using EPR and optical spectroscopy. With this approach it was possible to demonstrate that the ligand is partially replaced by DMF molecules. Thus, an equilibrium between different species exists. This behaviour is not unexpected in oxygen-containing solvents.

In the case of the copper complexes, the major paramagnetic species present in DMF are four-co-ordinate components with tetrahedral distorted square-planar geometry around the copper ion and with the counter ions participating in the inner sphere of co-ordination.

In the case of the iron complexes the mixture of the paramagnetic species present in DMF solutions involves monomers with high-spin Fe^{3+} in an octahedral co-ordination and with very different rhombicity.

Both metals are co-ordinated by two nitrogen atoms of the substituent in the 3-position of phenothiazine, as indicated in Fig. 6. Thus a direct interaction between the phenothiazine moiety and the metal does not seem to be required for the pharmacological activity of these compounds.

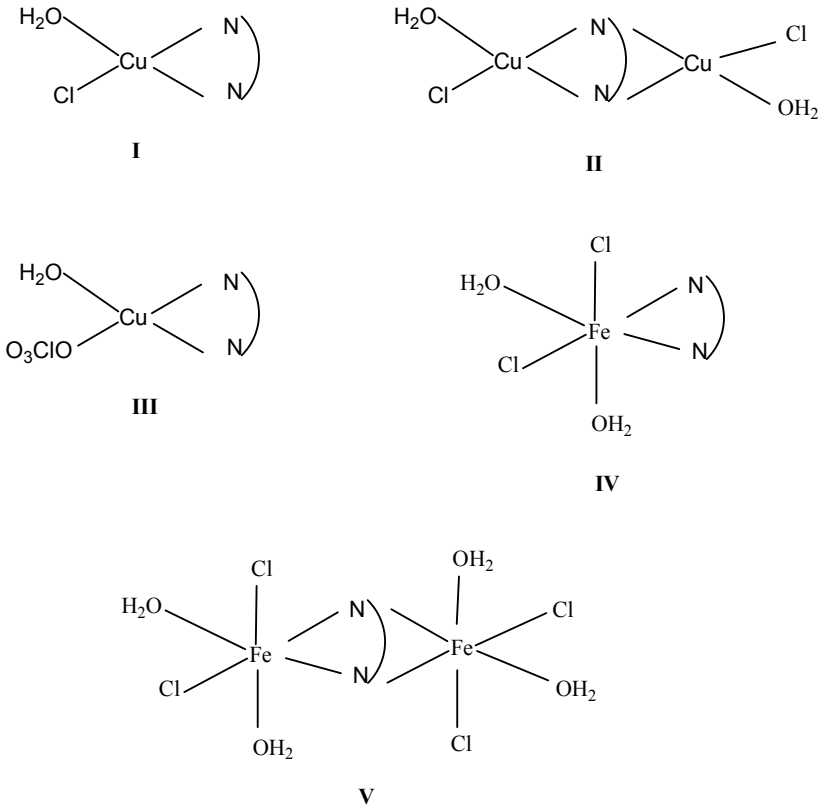

Fig. 6 – Proposed structures for **I**, **II**, **III**, **IV** and **V** complexes.

Further separation of the major species as well as the change of the factors involved in the complexes formations (concentration, pH or solvent), are necessary to understand the relation between the first-sphere co-ordination of the metal and its biological activity.

REFERENCES

1. S. Chang, V.V. Karambelkar, R.C. diTargiani and D.P. Goldberg, *Inorg. Chem*., **2001**, *40*, 194.
2. P.S. Subramanian, E. Suresh, P. Dastidar, S. Waghmode and D. Srinivas*, Inorg. Chem*., **2001**, *40*, 4291.
3. N. Motohashi, T. Kurihara, K. Satoh, H. Sakagami, I. Mucsi, R. Pusztai, M. Szabo and J. Molnar, *Anticancer Res*., **1999**, *19*, 1937.

4. V.M. D'Souza and V. Yayarama, *Indian J. Chem.*, **1986**, *25A*, 183.
5. P.G. Ramappa, *J Indian Chem. Soc*., **1999**, *76*, 235.
6. C. Guran, E. Bacu, I. Ciocoiu, N. Carp, V. Iluc, P. Diaconescu, M. Bon and S. Nicolae, *Roum. Biotechnol. Lett*., **1998**, *3*, 123.
7. M. Tanaka, J. Molnar and S. Kidd, *Anticancer Res*., **1997**, *17*, 381.
8. K. Pierloot, J.A.P. De Kerpel, U. Ryde, H.M. Olsson and B.O. Roos, *J. Am. Chem. Soc.*, **1998**, *120*, 13156.
9. F. Capozzi, S. Ciurli and C. Luchinat, *Structure and bonding*, Springer Verlag, **1998**, *90*, 127.
10. V. Schuenemann, A.X. Trautwein, J. Illerhaus and W. Haehnel, *Biochemistry*, **1999**, *38*, 8981.
11. I.S. Ahuja and S. Tripathi, *Synth. React. Inorg. Met.- Org. Chem*., **1992**, *22*, 1251.
12. S. Pasolescu, C. Guran, I. Ciocoiu and E. Bacu, *Rev. Roum. Biochim*., **2002**, in press.
13. J.A. Hafen, J.M. Uhan, D.C. Fox, M.P. Mehn and L.Que, *Inorg. Chem*., **2000**, *39*, 4913.
14. C.T. Jang, B. Moubaraki, J.D. Murray, J.D. Randford and J.J. Vittal, *Inorg.Chem.*, **2001**, *40*, 5934.
15. B.J. Hathaway, in "Comprehensive Coordination Chemistry", R.D. Wilkinson and J.A. Giles Eds., McCleventry, Pergamon Press, Oxford, 1987, Vol. 5.
16. H. Yokoi and A.W. Addison, *Inorg. Chem*., **1977**, *16*, 1341.
17. S. Parimala, K.N. Gita and M. Kandaswamy, *Polyhedron*, **1998**, *17*, 3445.
18. B.J. Hathaway, in "Structure and Bonding", Springer Verlag, 1984, *57*, 55.
19. K. Fukumaru, T. Sawada, N. Nishino and H. Sakurai, *Chem. Pharm. Bull*., **1996**, *44*, 1989.
20. A.E. Palmer, D.W. Randall, F. Xu and E.I. Solomon, *J. Am. Chem. Soc*., **1999**, *121*, 7138.
21. R. Basosi, *4th Meeting of European Federation of EPR Groups*, Norwich, **2000**, L24.
22. K. Ramesh and R. Mukherjee, *J.Chem. Soc.Dalton Trans*, **1992**, 83.
23. W.R. Hagen, *Adv. Inorg. Chem*., **1992**, *38*, 165.
24. M. Maltempo and M.E. Eberhard, *Chem. Phys. Lett*., **1984,** *108*, 204.
25. J. Costa, R. Delgado, M.G.B. Drew, V. Felix, R.T. Henriques and J.C. Waerenborgh, *J. Chem. Soc. Dalton Trans,* **1999**, 3253.
26. G. Batra and P. Mathur, *Polyhedron,* **1993**, *12*, 2635.
27. R.M. Golding, M. Kestigian and C.W. Tennant, *J. Phys. C,* **1978**, *11*, 5041.
28. E. Bâcu, *Doctoral Thesis*, Dep. of Org.Chem., University "A.I.Cuza", Iaşi, **1996**.
29. S. Pasolescu, C.G. Palivan and C. Guran, *Polyhedron,* **2002**, in press.
30. Symfonia software, Bruker, **1992**.
31. I. Bertini, D. Gatteschi and C. Zanchini, *J. Am. Chem. Soc*., **1980**, *102*, 5234
32. J. A. Halfen,, J. M. Uhan, D. C. Fox, M. P. Mehn, and L. Que Jr., *Inorg.Chem.*, **2000**, *39*, 4913-4920.
33. C.Gerarda, A. Mohamadou, J.Marrotb, St. Brandesc and Alain Tabardc, *Helvetica Chimica Acta*, **2005,** *88*, 2392.